Chemical Engineering Journal 152 (2009) 575–582

Contents lists available at ScienceDirect

Chemical Engineering Journal

journal homepage: www.elsevier.com/locate/cej

Design and simulation of passive mixing in microfluidic systems with geometric variations

Wonjin Jeon, Chee Burm Shin*

Dept. of Chemical Engineering and Division of Energy Research Systems, Ajou University, Suwon 443-749, Republic of Korea

ARTICLE INFO

Article history:
Received 20 February 2009
Received in revised form 21 May 2009
Accepted 22 May 2009

Keywords:
Microfluidics
Micro-mixers
Passive mixing
Obstructive structure
Gold nano-particles aggregation

ABSTRACT

Miniaturized systems based on the principles of microfluidics are widely used in various fields, such as biochemical and medical applications. Systematic design processes are demanded for the proper use of these microfluidic devices based on mathematical simulations. In this research, passive mixing, without external forces, was simulated and analyzed with Fluent 6.1. After the simulation process, PDMS-based micro-chips were fabricated for use in experiments. In the experiments, gold nano-particles and $CuSO_4$ solutions were used to visualize their mixing tendencies. Because the gold nano-particles were composed of specific aggregations with metal ions, colorimetric variations could be detected by the naked eye without any optical equipment. The simulation results showed good agreement with the experimental ones. The pressure drop in the micro-mixers was small and, therefore, their structures were deemed to be suitable for integration with lab-on-a-chips or micro-total analysis systems.

1. Introduction

Microfluidic systems have attracted a great deal of attention in a range of fields as diverse as physics, chemistry, biology, medicine and engineering. Miniaturized systems, such as micro-total analysis systems (μTASs) and lab-on-a-chips (LOCs), are suitable for cases requiring a small amount of reagent. Microfluidic systems will be indispensable for reducing the experimental cost if the prices of the reagents become too expensive for some biological experiments. In addition, their low production cost, reduced reaction time, portability and the multiplicity of design are the general merits of micro-scale systems [1]. However, mixing is a crucial factor for the performance of microfluidic devices, because of their low Reynolds numbers. Previous reviews on micro-mixers are given in Refs. [1–4]. Mixing at the micro-scale can be classified into passive mixing and active mixing. In passive mixing, external energy is not required but diffusion or chaotic advection induces mixing. Parallel lamination [5,6], serial lamination [7,8] and interdigital multi-lamination [9,10] provide fast mixing by decreasing the mixing path and increasing the contact surface between the mixing phases. Chaotic advection can be generated by special geometries in the mixing channel. Examples are obstacles on the wall of flow channel [11,12], obstacles in the flow channel [13,14] and zigzag channel [15]. Similar works have been studied extensively both numerically and experimentally to enhance the convective heat transfer in micro-channels with various fin arrangements [16–18]. Injection of substreams via nozzles into main stream presents a means for mixing [19]. In active mixing, external energy is used for the mixing process. Examples of external energy sources are micropumps [20,21], ultrasound [22] and acoustically induced vibrations [23,24] and electro-hydrodynamic [25] and magneto-hydrodynamic actions [26] among others. However, the integration of external power sources in a microfluidic system often requires complex fabrication processes. In contrast, the passive mixers are stable in operation and easily integrated in a complex microfluidic system. Although the processes of design and fabrication of passive systems are generally known to be simpler than those of active ones, the flow control is a critical problem in these systems [27]. Therefore, the optimum design of passive mixing systems is very important and needs a preprocessing step, such as a mathematical simulation [27,28]. In a passive mixing LOC, the flow stream is controlled by adjusting its dimensions, such as the height, length and width, because of the absence of any external power resource [29]. Thus, careful consideration of the design of the micro-channels and obstructions is essential to raise the passive mixing performance. The fundamental principles of microfluidic systems focus on the behavior of fluids in microfluidic channels, and the Reynolds number (Re) can be used to define their behavior [30]. The flow instability that induces disturbed flow is determined by the Reynolds number, $Re = lv\rho/\mu$ where l is the most relevant length scale, μ is the viscosity, ρ is the fluid density, and the v is the average velocity of the flow, which means the ratio of the inertia forces to the viscous forces in the fluid stream. The Reynolds number regime is a crucial factor influencing the design of microfluidic systems. Due to the micro-scale dimensions of the design, the

* Corresponding author. Tel.: +82 31 219 2388; fax: +82 31 219 1612.
E-mail address: cbshin@ajou.ac.kr (C.B. Shin).

1385-8947/$ – see front matter © 2009 Elsevier B.V. All rights reserved.
doi:10.1016/j.cej.2009.05.035

Reynolds number is generally <100 or may even approach 1. In this case, the flow is fully laminar and there is no turbulence within it. A transition from laminar flow to turbulent flow generally occurs when the Reynolds number exceeds 2000. In the regime of laminar flow, the behavior of the micro-scale flow is predictable to a certain extent, because of its slow and uniform flow tendency. Its behavior can be predicted more precisely and reasonably by mathematical simulation [29,31].

Along with mathematical simulations, micro-scale flow visualization plays an important role for understanding microfluidic flows to develop novel microfluidic devices. Regular fluorophores such as fluorescein are commonly used in direct visualization of mixing in microfluidic devices [29,32]. Matsumoto et al. measured optically a depth-averaged concentration fields in a liquid micro-channel flow [33]. In order to get the three-dimensional information of the concentration field with high spatial resolution, confocal laser scanning microscopy (CLSM) should be used [34]. Park et al. repeated scanning for multiple focal planes to reconstruct three-dimensional images [35]. Yamaguchi et al. used confocal microscopy to visualize fluorescent intensity patterns in micro-channels and compared them with the results from computational fluid dynamics [36]. The microscopic particle image velocimetry (μ-PIV) has been successfully adapted for measuring flow fields within microfluidic devices. Hsieh and Huang studied passive planar micro-mixers with geometric variations through microscopic laser-induced fluorescence and μ-PIV [31]. Park et al. applied CSLM in connection with μ-PIV and showed a unique optical slicing capability allowing true depth-wise resolved μ-PIV vector field mapping [35].

In this study, various passive mixing systems with low Reynolds numbers near to 1 were designed, simulated and fabricated to obtain efficient mixing performance. To verify the simulated results, a small amount of solution with gold nano-particles (Au NPs) was used in the tests. The specific character of the colorimetric reaction between two solutions was expected to reveal the mixing tendency to the naked eye. This method does not need additional equipment for observation. To optimize the performance of the microfluidic devices, a mathematical simulation was conducted based on three-dimensional meshes. The AutoCAD 2006 and Fluent 6.1 software programs were used in the design and simulation processes, respectively. To fabricate the microfluidic systems, polydimethylsiloxane (PDMS) was used and the fabricated devices had planar shapes. The driving force was only the capillary force in the micro-channels.

2. Micro-chip design

The passive microfluidic systems were designed to operate by capillary force. Therefore, natural flow from the inlets to the micro-channels was necessary, without any additional external forces. When 200 μl of two sorts of solutions were injected into each inlet in drops, the solutions flowed in the micro-channels and mixed together. Fig. 1 shows the schematic geometries of the proposed passive micro-mixers. In this paper, the investigation was focused on the passive mixers within the red rectangular region, because the overall performance of the system is dependent on the pre-mixing of the passive mixers. The wavy channel on the left-hand side of the total structure was proposed to control the residence time of the solutions. The obstructions and winding channels in the pre-mixing zones were expected to induce more effective mixing performance than the basic type, which had no baffles or winding channels. The velocity profiles, such as the velocity and direction, were expected to variously change near the obstructions.

The width and height of the mixer were 10.6 mm and 38.9 mm, respectively. The depth of the mixers was 10 μm and the length scales of all of the mixers were equal, except for the obstructions. For the obstructions, in Fig. 1(a)–(c), the area of all of the baffles was

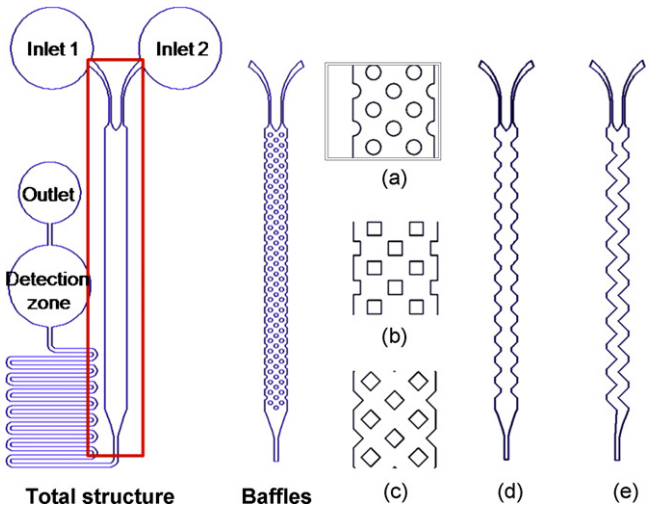

Fig. 1. Various schematic geometries of micro-mixers with obstructions or winding: (a) circular type, (b) rectangular type, (c) rhombic type, (d) contraction-enlargement type and (e) zigzag type.

equal, although they each had different shaped baffles, viz. circular, rectangular and rhombic. The diameter of the circular baffle was 0.4 mm and the length of the edges of the rectangular and rhombic baffles was 0.3536 mm. The distances between the centers of the baffles were equal in all three types. The horizontal distance between the two centers of the baffles was 1.08 mm. The vertical and diagonal distances were 1 mm and 0.73 mm, respectively. For the contraction-enlargement type, the contracting width was 1.0 mm and the enlarging width was 2.16 mm. Continuous variations of the velocity of the flow streams occurred and effective mixing was induced in this micro-mixer. The width of the micro-channel of the zigzag type was 1.0 mm and the curved angle was 90°. Sudden changes of the flow direction were expected to occur in the zigzag type of mixer.

3. Methods

3.1. Numerical simulation

Fluent 6.1 (Fluent Inc.) was used to carry out the three-dimensional simulation in this study. Fluent is a comprehensive tool for computational fluid dynamics and is widely used in many engineering fields, such as aerospace, fluidics and even semiconductor manufacturing. In the microfluidics field, this tool is used in a wide range of activities and provides reasonable performance [36–38]. In addition to Fluent, other simulation tools are also used in microfluidics studies, such as COMSOL [39], ANSYS-CFX5 [40], CFD-ACE [41] and FEMLAB [42]. Fluent provides comprehensive modeling capabilities for a wide range of incompressible and compressible, laminar and turbulent fluid flow problems. In addition, it also provides reasonable solutions for the steady or transient states. The regime of microfluidic devices developed in this paper was included in the lamina region ($Re \ll 2100$) [43], and the reagents were incompressible liquids containing particles. For these conditions, Fluent was selected as the simulator of choice in this study.

Mixture model involved in multiphase models of Fluent was used to obtain Au NPs distributions and velocity profiles. The mixture model is suitable for simulating the transport of two or more sorts of particles in liquids, and the phases are treated as interpenetrating continua. The mixture model solves the mixture momentum equation and sets relative velocities to describe the dispersed phases. The phases were composed of water, Au NPs and a target material to be detected by the Au NPs. The target material

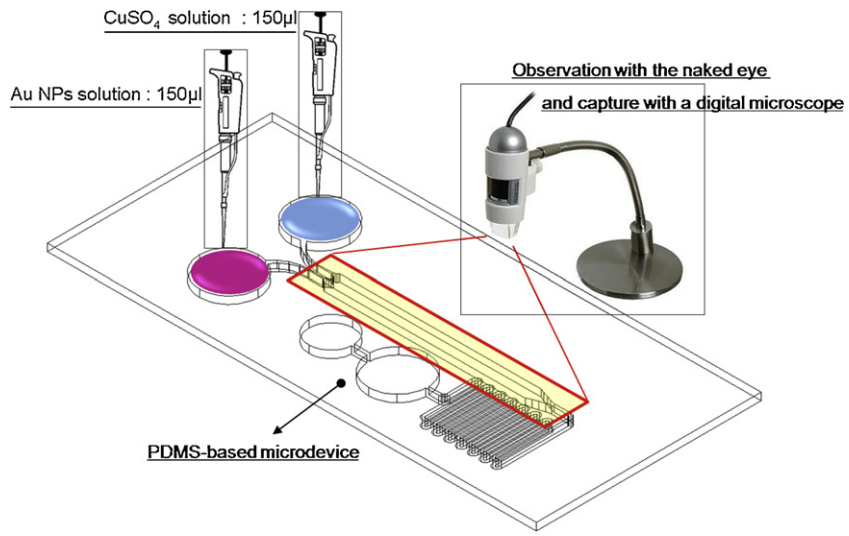

Fig. 2. Schematic diagram of the experimental method of observing the colorimetric variations. The digital micro-scope was focused on the micro-mixer part and recorded the micro-flow in the mixer in real-time. The practical flow velocity was lower than the simulation parameter (2–3 mm/s).

was assumed to be a hypothetical substance reacting with the Au NPs which could be metal ions or bio-samples such as proteins. The initial velocities of the inflow from the two inlets were assumed to be 3 mm/s and the initial volume fractions of the Au NPs and the target material were set to 0.1. The target material was assumed to be an arbitrary material having the shape of complete spheres and a density of 1500 kg/m^3. The diameters of the target material and Au NPs were specified as 4 nm and 20 nm, respectively. The boundary condition for the inner walls of the micro-channels was defined as the no slip condition for the sake of simplicity [36]. The total number of meshes was about 83,000 sections with an interval of 0.05 μm.

3.2. Fabrication method

The fabrication processes were composed of mold fabrication, chip fabrication, and surface treatment. In the mold fabrication process, a 4 in. silicon wafer was used as the substrate. SU-8 2000

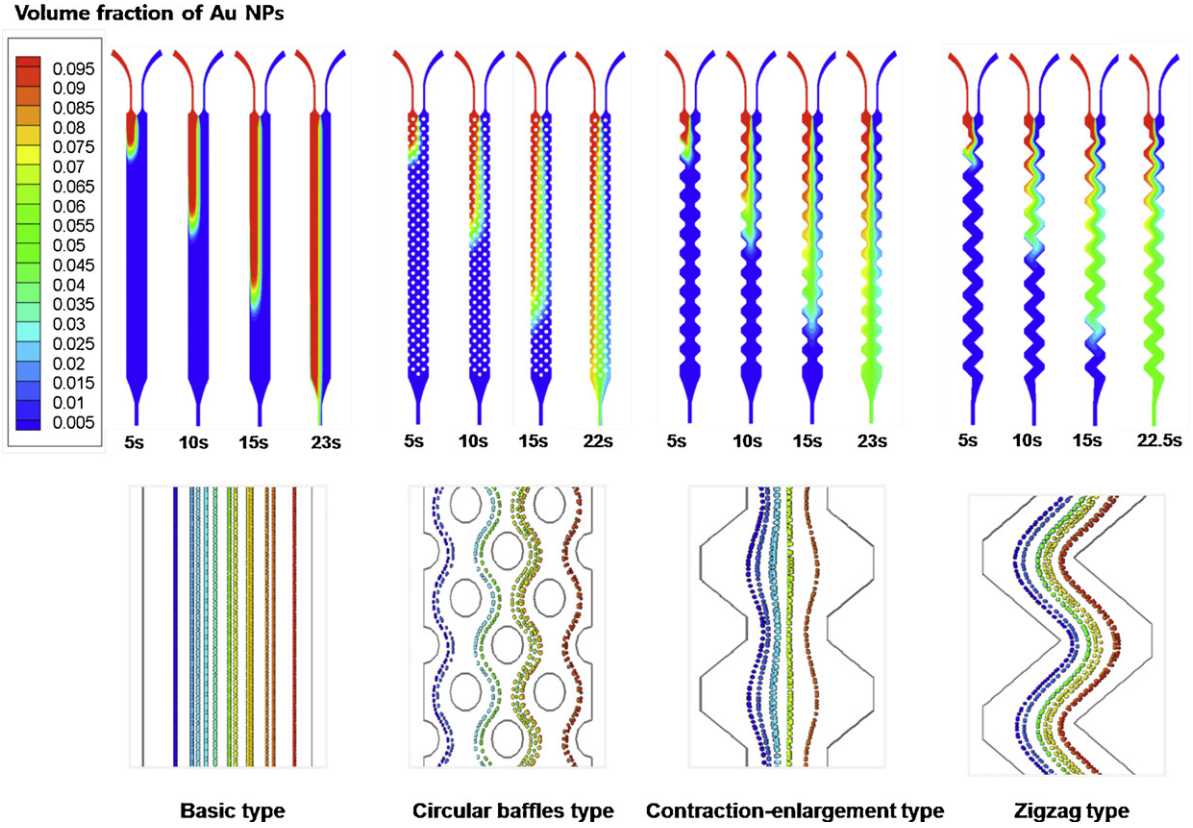

Fig. 3. Contours of volume fraction of Au NPs and path lines of particles in different micro-mixers in unsteady state. A green color on the contour plot is an indication of the even dispersion of the Au NPs. The plot of path lines was colored by particle ID in Fluent 6.1. (For interpretation of the references to color in this figure legend, the reader is referred to the web version of the article.)

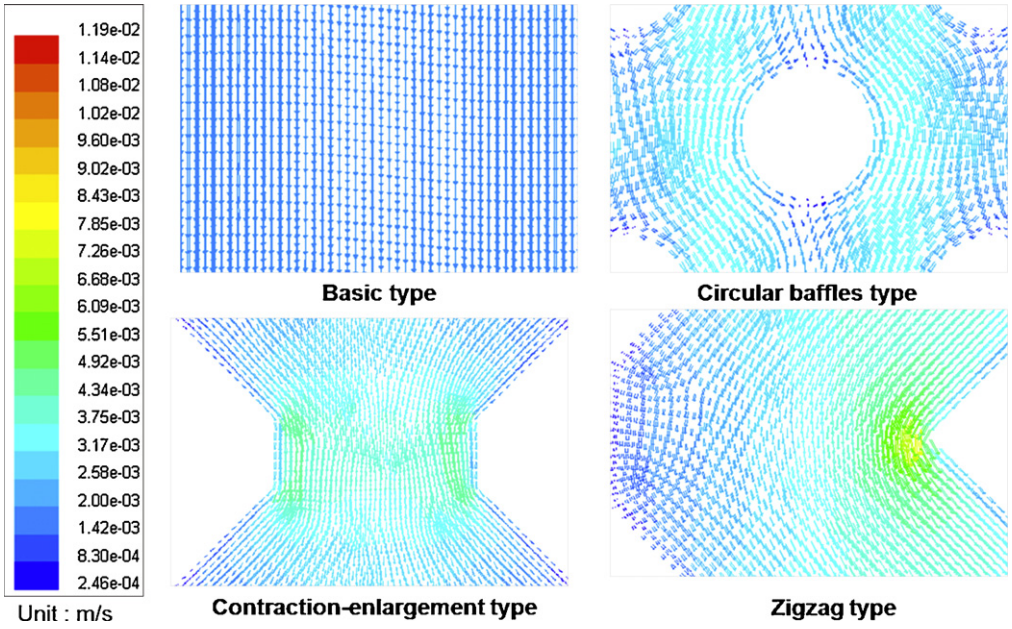

Fig. 4. Velocity profiles of mixtures in different micro-mixers with vectors and contours. The velocity variations were observed near the obstructive locations. The unit of velocity was meters per second.

was used as a photoresist material (MicroChem Inc.) and micro-patterns of PDMS were generated on the substrate by a replica molding method [44]. In the fabrication processes, polydimethylsiloxane (PDMS) was the basic component of the microfluidic devices. A Sylgard 184 kit (Dow Corning Corporation) containing PDMS pre-polymer (Sylgard 184-A) and curing agent (Sylgard 184-B) was employed. The pre-polymer has the physical form of a colorless liquid with a specific gravity and viscosity at 25 °C of 1.11 and 5000 cSt, respectively. The curing agent is also a colorless liquid with a specific gravity and viscosity at 25 °C of 1.03 and 110 cSt [45], respectively. PDMS based materials have many advantages for biological analysis [44], which include a low production cost, non-toxicity, reversible deformation and an optically clear surface.

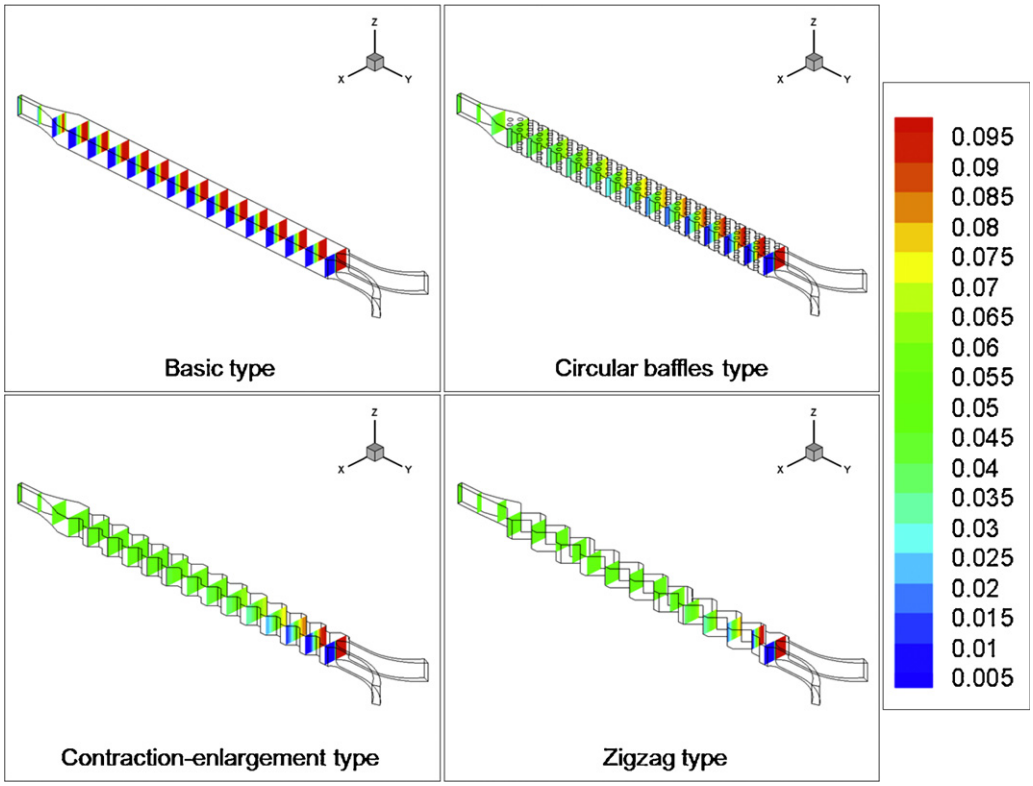

Fig. 5. Cross-sectional distributions of volume fraction of Au NPs in micro-mixers. The pure blue and red regions gradually decreased at the lower positions in all of the micro-mixers except for the basic type. The pure blue and red colors indicated the pure Au NPs and $CuSO_4$ solutions, respectively. (For interpretation of the references to color in this figure legend, the reader is referred to the web version of the article.)

Using the completed mold, PDMS based devices were fabricated through a series of steps. The pre-polymer and curing agent were mixed on a square dish at a weight ratio of 10:1 for 5 min. After mixing, the mixture with many bubbles was positioned in a vacuum oven at 40 °C for 1 h. The bubbles escaped from the mixture through this degassing process. The mixture was then baked in an oven at 70–80 °C for 1 h. After the PDMS based chips were fabricated, their surface was cleaned with acetone in an ultrasonicator for 5 min.

The pure PDMS surface after curing was quite hydrophobic. However, the completed microfluidic devices need to be used with hydrophilic solutions, such as water or a buffer solution. Therefore, the surface should be treated to render it hydrophilic for the sake of ensuring smooth flow. To increase the hydrophilic properties of the cured PDMS surface, surface treatment was carried out with an RF plasma and a functional solution, viz. hydroxyethyl methacrylate (HEMA, CAS: 868-77-9). The hydroxyethyl methacrylate (Samchun Chemical Inc.) solution was used as a surface modifier [46,47]. It is a colorless liquid with the systematic formula, $H_2C{=}C(CH_3)COOCH_2CH_2OH$. Its boiling point is 67 °C at 3.5 mmHg and its vapor pressure at 25 °C is 0.01 mmHg. The RF

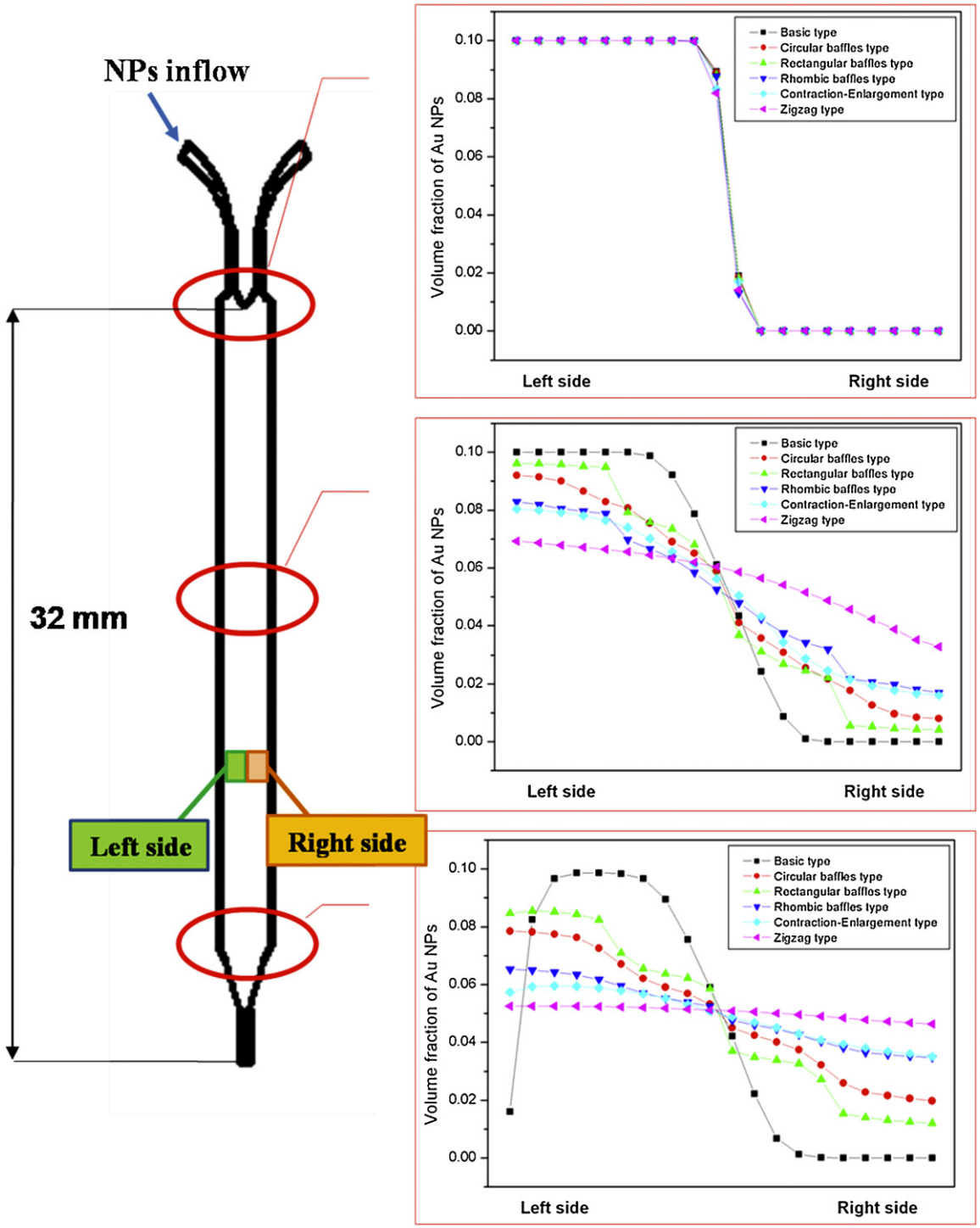

Fig. 6. Distribution of Au NPs across the channel cross-section in the simulation at various positions. The contours in Fig. 5 were quantified to recognize slight differences of the mixing effect.

plasma was induced with a power of 100 W for 15 min. Initially, the oxygen plasma modified the cured PDMS surface with a pressure of 100 bars and flow rate of 20 sccm. The RF power was 100 W and the exposure time was 30 s. Then, the surface was coated with HEMA by a spin coating method at 1500 rpm. Finally, the oxygen plasma treatment was performed under the same conditions for 5 min.

3.3. Experimental observations

Protein aggregation is one of the key elements of the biophysical stability of a protein, as well as a pathological feature of many disorders in the human body. As an example, the aggregated structure of superoxide dismutase (SOD1) in motor neurons is a key feature of the pathology of both sporadic and familial amyotrophic lateral sclerosis (ALS) [48]. Hong et al. reported the Au NP-based highly sensitive and colorimetric detection of the temporal evolution of SOD1 aggregates [49]. This property provides the potential to develop a novel microfluidic device for the diagnosis of ALS. As a preliminary study, we observed the colorimetric variations induced by the mixing of the solutions containing Au NPs and a target material in a microfluidic system. In this study, $CuSO_4$ solution was selected as the target material, as shown in Fig. 2. The aggregation of Au NPs with copper ions results in a colorimetric response and makes the mixture of two solutions increasingly darker over time [50]. The diameter of the Au NPs was 20 nm and the concentration of $CuSO_4$ was 100 mM. The Au NPs and $CuSO_4$ were dissolved in deionized water. 150 μl each of the Au NPs and $CuSO_4$ solutions were simultaneously injected into the two inlets. Because the purpose of this study was the observation of the colorimetric variations by the naked eye, a commercial digital micro-scope (AM311S – DinoLite, AnMo Electronics Inc.) was used to record the flow patterns and tendencies from the same viewpoint as that of the naked eye. The other mixing test reactions such as the Dushman reaction proposed once by Villermaux and coworkers [51] which may provide quantitative information on mixing were not used, since the main purpose of this study was to test the feasibility of the microfluidic device based on the colorimetric variation of the solution containing Au NPs.

4. Results and discussion

The three-dimensional simulation with Fluent 6.1 provided the mixing tendencies of the two solutions in the different micro-mixers, as shown in Fig. 3. We presented the dynamic inlet flow behaviors at the start-up stage and those are not the steady-state flow behaviors. Using these contours, the degrees of mixing of the micro-flows could be estimated from their shapes. To ensure a reasonable analysis, the contours were selected and compared at the point in time when the volume fraction first reached 0.05 at each outlet in the case of all of the micro-mixers. In the case of the basic type without any modification, the Au NP solution from the left inlet did not disperse and flowed parallel with the flow of the target solution. Because of its simple geometry, there was no mixing and the solutions just straightly flowed through the micro-mixer. On the other hand, in the three micro-mixers with circular, rectangular and rhombic obstructions, respectively, more effective dispersion of the Au NPs was simulated than in the basic one. The three types of mixers had similar dispersion tendencies in their contours and the circular case is shown in Fig. 3. The driving force of mixing in the circular type micro-mixer was based on the variations of the flow direction, as shown in the path lines in Fig. 3. The no slip boundary condition influenced the direction and velocity of flow near the surfaces of the baffles. The micro-mixers with contraction-enlargement and zigzag shapes also showed more effective mixing performance than the basic type. The direction of the path lines in these two micro-mixers also varied continuously. The variations of velocity and pressure through the repeatedly contracting and enlarging channel were the driving force for mixing in the contraction-enlargement type micro-mixer. In the zigzag type micro-mixer, the channel with a curvature of 90° influenced the flow direction and velocity at the inner and outer corners of the channel, as shown in Fig. 4.

The effective mixing performance is expected between the Au NPs and target solution as the Au NPs evenly dispersed in the micro-mixers. The green color, with a value of 0.5, on the contour plot is an indication of the even dispersion of Au NPs. The cross-sectional contours in Fig. 5 clearly showed the differences of the mixing tendencies. Red and blue regions should disappear in the case of effective mixing. However, in the basic type of mixer, the red and blue zones remained near the outlet of the mixer. Among the various micro-mixers, the zigzag type included the most homogeneous green regions and, thus, this type of micro-mixer was expected to have the best mixing performance in the simulation. However, quantitative analysis of the simulation results is needed to compare the various cases precisely.

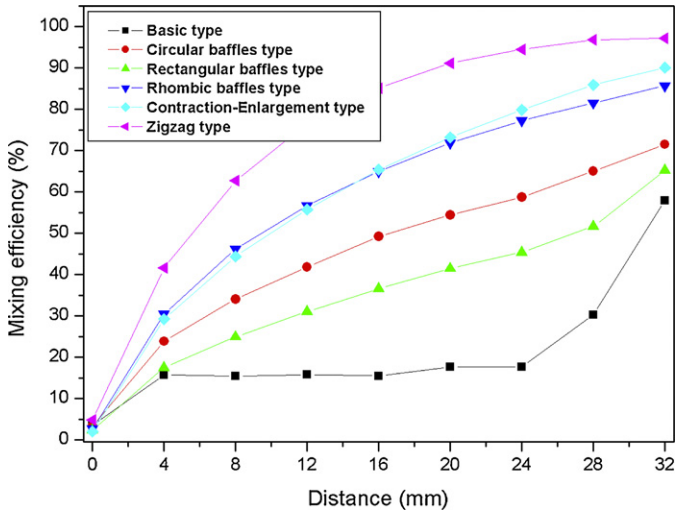

Fig. 7. Simulation of mixing efficiencies in different micro-mixers. The basic type showed the lowest mixing efficiency and the rhombic type provided higher mixing efficiency than the other similar types of mixers with circular or rectangular baffles.

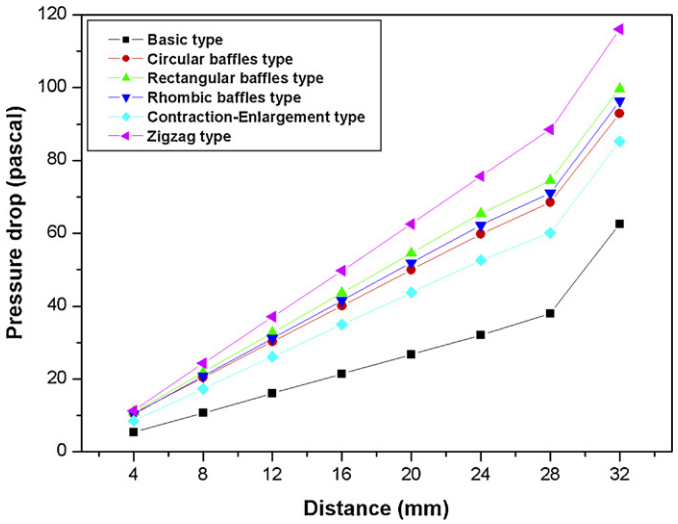

Fig. 8. Simulation of pressure drop in different micro-mixers. The basic type incurred the smallest pressure drop, because of its straight structure without any obstructions. The pressure drop in the zigzag type was the largest, due to the drastic change of the flow direction induced by its curved geometry.

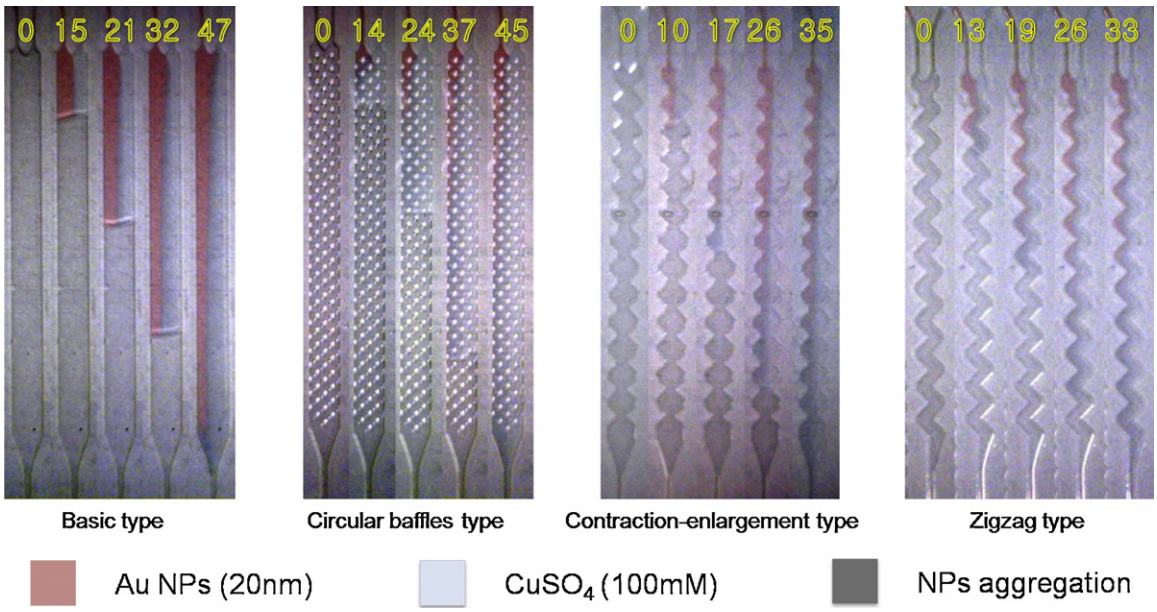

Fig. 9. Observation of mixing tendencies of different micro-mixers by the naked eye. The captured photographs showed good agreement with the contours determined by simulation. All of the micro-mixers except the zigzag type showed biased mixing flows. The numbers on the top of the photographs indicate the elapsed time in seconds from the start-up.

In Fig. 6, the quantitative plots of the distribution of the Au NPs are displayed for specific positions, viz. the upper, middle and lower parts. As the differences in the volume fractions between the left and right sides were small, the mixing was effective. In the upper part, there was no mixing, because all of the micro-mixers had the same geometry without obstructions. As the target position moved downward, different degrees of mixing were observed depending on the shapes of the mixers. The zigzag type of micro-mixer had the best mixing performance and this result corresponded with the conclusion reached based on the contours. Based on the quantitative simulation results, the mixing efficiency was evaluated at the different positions, from the upper to lower locations. The mixing efficiency was defined as:

$$m_{eff} = \left(1 - \frac{\int_0^w |v - v_\infty| dx}{\int_0^w |v_0 - v_\infty| dx}\right) \times 100\% \quad (1)$$

where m_{eff} is the mixing efficiency, v is the volume fraction distribution across the transverse direction at the outlet, v_∞ is the volume fraction of complete mixing, v_0 is the initial distribution of the volume fraction before any mixing occurs and W is the width of the micro-mixers [31]. To evaluate the mixing efficiency based on the volume fraction of Au NPs, the concentration terms in the original expression were substituted for the volume fraction in Eq. (1). Based on the data in Fig. 6, the mixing efficiencies of the various micro-mixers were calculated for the transverse locations and the results are shown in Fig. 7. The distribution of the mixing efficiency showed similar tendencies to the former simulation results. The zigzag type micro-mixer provided the most effective mixing and the basic type without obstructions showed the least mixing. Although the basic type micro-mixer generally showed the worst mixing performance, the value of the basic type micro-mixer drastically increased at the last location. This may be the benefit of hydrodynamic focusing due to the funnel-shaped outlet. In Fig. 8, the pressure drops in the micro-mixers are evaluated. As shown in Fig. 8, the pressure drop in the basic type micro-mixer was the smallest, because of its simple geometry. However, the other micro-mixers provided larger pressure drops than the basic one due to their modified structures. Among them, the zigzag type provided the largest pressure drop. The reason for this was likely that the overall flow direction changed most drastically with an angle of 90°. The pressure drop in the zigzag mixer was larger than those of different types, but its value was not very large and would be suitable for overall passive micro-mixers [29]. A high mixing efficiency and low pressure drop are essential factors for applications, such as the integration of LOCs [51–54].

Practical mixing in the micro-mixers was observed by the naked eye and recorded by the commercial digital micro-scope from the same viewpoint as that of the observers. The observation results of the mixing of the two reagents are presented in Fig. 9. The pink stream is the Au NPs solution and the pale blue stream is the $CuSO_4$ solution. If the two solutions completely mixed, the mixture involving Au NPs aggregations had a dark color [50]. In Fig. 9, analogous tendencies of the mixing patterns are observed compared with the contours determined by the mathematical simulation. As expected, the mixing in the basic type micro-mixer was ineffective. The circular type and contraction-enlargement type micro-mixers showed more capable mixing, but the dark regions were biased to the left side of the micro-mixers. However, the dark region of aggregations was homogeneously distributed in the zigzag mixer. This result corresponded with the simulation results shown in Fig. 6. This correspondence indicated that the zigzag type of micro-mixer had the most effective mixing performance.

5. Conclusions

In this study, the effective mixing performance of passive planar micro-mixers with different geometries was investigated by the simulation and experiments. The microfluidic devices were simply designed to operate with only capillary force. The obstructive structures induced the efficient mixing of the reagents in the simulation with a low Reynolds number (Re < 1). The simulation of passive mixing in the planar micro-mixers was achieved using Fluent 6.1. In the fabrication based on PDMS, it was simple and easy to fabricate the devices without complicated 3D structures. The modification of the surface to render it hydrophilic was essential to ensure the smooth flow of the aqueous solutions without additional equipment, such as micro-pumps. The experiments with Au NPs and $CuSO_4$ solutions showed good agreement of the mixing tendencies with the simula-

tion results. The colorimetric observation of the mixing effects with the devices was very simple, economic and time saving, because it demanded just a few hundred micro-liters of input solutions, without the need for any fluorescent equipment. Moreover, the micro-mixers incurred a small amount of pressure drop and, thus, have the potential to be integrated with other microfluidic systems. Research into LOC involving nano-particles has been actively pursued in the biological, chemical and physical fields. Therefore, the method of analyzing the mixing performance described in this paper is expected to provide valuable guidelines for mixer design with various nano-particles.

Acknowledgements

The authors acknowledge the Korea Science and Engineering Foundation (KOSEF 2009-0064626) and the Ministry of Knowledge Economy of Republic of Korea (2007-E-1D25-P-02-0-00) for providing financial supports for this work.

References

[1] N.T. Nguyen, Z. Wu, Micromixers—a review, J. Micromech. Microeng. 15 (2005) R1–R16.
[2] V. Hessel, H. Löwe, F. Schönfeld, Micromixers—a review on passive and active mixing principles, Chem. Eng. Sci. 60 (2005) 2479–2501.
[3] S. Hardt, K.S. Drese, V. Hessel, F. Schönfeld, Passive micromixers for applications in the microreactor and μTAS fields, Microfluid Nanofluid 1 (2005) 108–118.
[4] C.J. Campbell, B.A. Grzybowski, Microfluidic mixers: from microfabricated to self-assembling devices, Philos. Trans. R. Soc. Lond. A 362 (2004) 1069–1086.
[5] D. Gobby, P. Angeli, A. Gavriilidis, Mixing characteristics of T-type microfluidic mixers, J. Micromech. Microeng. 11 (2001) 126–132.
[6] A. Soleymani, E. Kolehmainen, I. Turunen, Numerical and experimental investigations of liquid mixing in T-type micromixers, Chem. Eng. J. 135S (2008) S219–S228.
[7] N. Schwesinger, T. Frank, H. Wurmus, A modular microfluid system with an integrated micromixer, J. Micromech. Microeng. 6 (1996) 99–102.
[8] M.S. Munson, P. Yager, Simple quantitative optical method for monitoring the extent of mixing applied to a novel microfluidic mixer, Anal. Chim. Acta 507 (2004) 63–71.
[9] V. Hessel, S. Hardt, H. Löwe, F. Schönfeld, Laminar mixing in different interdigital micromixers. I. Experimental characterization, AIChE J. 49 (2003) 566–577.
[10] S. Hardt, F. Schönfeld, Laminar mixing in different interdigital micromixers. II. Numerical simulations, AIChE J. 49 (2003) 578–584.
[11] S.H. Wong, P. Bryant, M. Ward, C. Wharton, Investigation of mixing in a cross-shaped micromixer with static mixing elements for reaction kinetics studies, Sens. Actuators B 95 (2003) 414–424.
[12] A.D. Stroock, S.K.W. Dertinger, A. Ajdari, I. Mezić, H.A. Stone, G.M. Whitesides, Chaotic mixer for microchannels, Science 295 (2002) 647–651.
[13] H. Wang, P. Iovenitti, E. Harvey, S. Masood, Optimizing layout of obstacles for enhanced mixing in microchannels, Smart Mater. Struct. 11 (2002) 662–667.
[14] Y. Lin, G.J. Gerfen, D.L. Rousseau, S.R. Yeh, Ultrafast microfluidic mixer and freeze-quenching device, Anal. Chem. 75 (2003) 5381–5386.
[15] V. Mengeaud, J. Josserand, H.H. Girault, Mixing processes in a zigzag microchannel: finite element simulations and optical study, Anal. Chem. 74 (2002) 4279–4286.
[16] Z.Y. Guo, Z.X. Li, Size effect on single-phase channel flow and heat transfer at microscale, Int. J. Heat Fluid Flow 24 (2003) 284–298.
[17] L. Li, G.P. Peterson, O. Cheng, Three-dimensional analysis of heat transfer in micro-heat sink with single phase flow, Int. J. Heat Mass Transfer 47 (2004) 4215–4231.
[18] P.X. Jiang, R.N. Xu, Heat transfer and pressure drop characteristics of mini-fin structures, Int. J. Heat Fluid Flow 28 (2007) 1167–1177.
[19] J.T. Coleman, J. McKechnie, D. Sinton, High-efficiency electrokinetic micromixing through symmetric sequential injection and expansion, Lab Chip 6 (2006) 1033–1039.
[20] T. Fujii, Y. Sando, K. Higashino, Y. Fujii, A plug and play microfluidic device, Lab Chip 3 (2003) 193–197.
[21] A. Glasgow, N. Aubry, Enhancement of microfluidic mixing using time pulsing, Lab Chip 3 (2003) 114–120.
[22] Z. Yang, H. Goto, M. Matsumoto, R. Maeda, Ultrasonic micromixer for microfluidic systems, Sens. Actuators A 93 (2001) 266–272.
[23] R.H. Liu, J. Yang, M.Z. Pindera, M. Athavale, P. Grodzinski, Bubble-induced acoustic micromixing, Lab Chip 2 (2002) 151–157.
[24] R.H. Liu, R. Lenigk, R.L. Druyor-Sanchez, J. Yang, P. Grodzinski, Hybridization enhancement using cavitation microstreaming, Anal. Chem. 75 (2003) 1911–1917.
[25] A.O. El Moctar, N. Aubry, J. Batton, Electro-hydrodynamic micro-fluidic mixer, Lab Chip 3 (2003) 273–280.
[26] J. West, B. Karamata, B. Lillis, J.P. Gleeson, J. Alderman, J.K. Collins, W. Lane, A. Mathewson, H. Berney, Application of magnetohydrodynamic actuation to continuous flow chemistry, Lab Chip 2 (2002) 224–230.
[27] C. Jen, C. Wu, Y. Lin, C. Wu, Design and simulation of the micromixer with chaotic advection in twisted microchannels, Lab Chip 3 (2003) 77–81.
[28] W. Lin, A passive grooved micromixer generating enhanced transverse rotations for microfluids, Chem. Eng. Technol. 31 (2008) 1210–1215.
[29] A.A.S. Bhagat, E.T.K. Peterson, I. Papautsky, A passive planar micromixer with obstructions for mixing at low Reynolds numbers, J. Micromech. Microeng. 17 (2007) 1017–1024.
[30] J.M. Ottino, S. Wiggins, Introduction: mixing in microfluidics, Philos. Trans. R. Soc. Lond. A 362 (2004) 923–935.
[31] S. Hsieh, Y. Huang, Passive mixing in micro-channels with geometric variations through μPIV and μLIF measurements, J. Micromech. Microeng. 18 (2008) 1–11.
[32] M.H. Oddy, J.G. Santiago, J.C. Mikkelsen, Electrokinetic instability micromixing, Anal. Chem. 73 (2001) 5822–5832.
[33] R. Matsumoto, H. Farangis Zadeh, P. Ehrhard, Quantitative measurement of depth-averaged concentration fields in microchannels by means of a fluorescence intensity method, Exp. Fluids 39 (2005) 722–729.
[34] M. Hoffmann, M. Schlüter, N. Räbiger, Experimental investigation of liquid–liquid mixing in T-shaped micro-mixers using μ-LIF and μ-PIV, Chem. Eng. Sci. 61 (2006) 2968–2976.
[35] J.S. Park, C.K. Choi, K.D. Kihm, Optically sliced micro-PIV using confocal laser scanning microscopy (CLSM), Exp. Fluids 37 (2004) 105–119.
[36] Y. Yamaguchi, F. Takagi, K. Yamashita, H. Nakamura, H. Maeda, K. Sotowa, K. Kusakabe, Y. Yamasaki, S. Morooka, 3D simulation and visualization of laminar flow in a microchannel with hair–pin curves, AIChE J. 50 (2004) 1530–1535.
[37] D.A. Boy, F. Gibou, S. Pennathur, Simulation tools for lab on a chip research: advantages, challenges, and thoughts for the future, Lab Chip 8 (2008) 1424–1431.
[38] P. Hinsmann, J. Frank, P. Svasek, M. Harasek, B. Lendl, Design, simulation and application of a new micromixing device for time resolved infrared spectroscopy of chemical reactions in solution, Lab Chip 1 (2001) 16–21.
[39] X. He, S. Hauan, Microfluidic modeling and design for continuous flow in electrokinetic mixing-reaction channels, AIChE J. 52 (2006) 3842–3851.
[40] J. Aubin, D.F. Fletcher, C. Xuereb, Design of micromixers using CFD modeling, Chem. Eng. Sci. 60 (2005) 2503–2516.
[41] C.K. Chung, C.Y. Wu, T.R. Shih, C.F. Wu, B.H. Wu, Design and simulation of a novel micro-mixer with baffles and side-wall injection into the main channel, in: Proceedings of the 1st IEEE International Conference on Nano/Micro Engineered and Molecular Systems, Zhuhai, China, 2006, pp. 721–724.
[42] A.J. Pfeiffer, X. He, T. Mukherjee, S. Hauan, A lab-on-a-chip simulation framework, in: Proceedings of the 16th European Symposium on Computer Aided Process Engineering and 9th International Symposium on Process Systems Engineering, Garmisch-Partenkirchen, Germany, 2006, pp. 1631–1636.
[43] C.J. Geankoplis, Transport Processes and Unit Operations, third ed., Prentice Hall PTR, New Jersey, 1993.
[44] J.C. McDonald, D.C. Duffy, J.R. Anderson, D.T. Chiu, H. Wu, O.J.A. Schueller, G.M. Whitesides, Fabrication of micro-fluidic systems in poly(dimethylsiloxane), Electrophoresis 21 (2000) 27–40.
[45] Material Safety Data Sheet of Sylgard 184 Silicone Elastomer Kit, Dow Corning Corporation, 2007.
[46] D. Bodas, C. Khan-Malek, Formation of more stable hydrophilic surfaces of PDMS by plasma and chemical treatments, Microelectron. Eng. 83 (2006) 1277–1279.
[47] D. Bodas, C. Khan-Malek, Hydrophilization and hydrophobic recovery of PDMS by oxygen plasma and chemical treatment—an SEM investigation, Sens. Actuators B 123 (2007) 368–373.
[48] E. Gaggelli, H. Kozlowski, D. Valensin, G. Valensin, Copper homeostasis and neurodegenerative disorders (Alzheimer's prion and Parkinson's diseases and amyotrophic lateral sclerosis), Chem. Rev. 106 (2006) 1995–2044.
[49] S. Hong, I. Choi, S. Lee, Y.I. Yang, T. Kang, J. Yi, Sensitive and colorimetric detection of the structural evolution of superoxide dismutase with gold nanoparticles, Anal. Chem. 81 (2009) 1378–1382.
[50] Y. Zhou, S. Wang, K. Zhang, X. Jiang, Visual detection of copper(II) by azide- and alkyne-functionalized gold nanoparticles using click chemistry, Angew. Chem. Int. Ed. 47 (2008) 1–4.
[51] M.-C. Fournier, L. Falk, J. Villermaux, A new parallel competing reaction system for assessing micromixing efficiency—determination of micromixing time by a simple mixing model, Chem. Eng. Sci. 51 (1996) 5187–5192.
[52] C.K. Chung, T.R. Shih, Y.S. Chen, C.H. Wang, Mixing process of an obstacles micromixer with low pressure drop, in: Proceedings of the 3rd IEEE Int. Conf. on Nano/Micro Engineered and Molecular Systems, Sanya, China, 2008, pp. 170–173.
[53] T.R. Shih, C.K. Chung, A high-efficiency planar micromixer with convection and diffusion mixing over a wide Reynolds number range, Microfluid Nanofluid 5 (2008) 175–183.
[54] C.K. Chung, T.R. Shih, A rhombic micromixer with asymmetrical flow for enhancing mixing, J. Micromech. Microeng. 17 (2007) 2495–2504.